BIOCHEMISTRY
including biophysical chemistry & molecular biology

Article

pubs.acs.org/biochemistry

Rate and Equilibrium Constants for an Enzyme Conformational Change during Catalysis by Orotidine 5′-Monophosphate Decarboxylase

Bogdana Goryanova,[†] Lawrence M. Goldman,[†] Shonoi Ming,[†] Tina L. Amyes,[†] John A. Gerlt,[‡] and John P. Richard*,[†]

[†]Department of Chemistry, University at Buffalo, State University of New York, Buffalo, New York 14260-3000, United States
[‡]Departments of Biochemistry and Chemistry, University of Illinois, Urbana, Illinois 61801, United States

ABSTRACT: The caged complex between orotidine 5′-monophosphate decarboxylase (*Sc*OMPDC) and 5-fluoroorotidine 5′-monophosphate (FOMP) undergoes decarboxylation ~300 times faster than the caged complex between *Sc*OMPDC and the physiological substrate, orotidine 5′-monophosphate (OMP). Consequently, the enzyme conformational changes required to lock FOMP at a protein cage and release product 5-fluorouridine 5′-monophosphate (FUMP) are kinetically significant steps. The caged form of *Sc*OMPDC is stabilized by interactions between the side chains from Gln215, Tyr217, and Arg235 and the substrate phosphodianion. The control of these interactions over the barrier to the binding of FOMP and the release of FUMP was probed by determining the effect of all combinations of single, double, and triple Q215A, Y217F, and R235A mutations on k_{cat}/K_m and k_{cat} for turnover of FOMP by wild-type *Sc*OMPDC; its values are limited by the rates of substrate binding and product release, respectively. The Q215A and Y217F mutations each result in an increase in k_{cat} and a decrease in k_{cat}/K_m, due to a weakening of the protein−phosphodianion interactions that favor fast product release and slow substrate binding. The Q215A/R235A mutation causes a large decrease in the kinetic parameters for *Sc*OMPDC-catalyzed decarboxylation of OMP, which are limited by the rate of the decarboxylation step, but much smaller decreases in the kinetic parameters for *Sc*OMPDC-catalyzed decarboxylation of FOMP, which are limited by the rate of enzyme conformational changes. By contrast, the Y217A mutation results in large decreases in k_{cat}/K_m for *Sc*OMPDC-catalyzed decarboxylation of both OMP and FOMP, because of the comparable effects of this mutation on rate-determining decarboxylation of enzyme-bound OMP and on the rate-determining enzyme conformational change for decarboxylation of FOMP. We propose that k_{cat} = 8.2 s^{-1} for decarboxylation of FOMP by the Y217A mutant is equal to the rate constant for cage formation from the complex between FOMP and the open enzyme, that the tyrosyl phenol group stabilizes the closed form of *Sc*OMPDC by hydrogen bonding to the substrate phosphodianion, and that the phenyl group of Y217 and F217 facilitates formation of the transition state for the rate-limiting conformational change. An analysis of kinetic data for mutant enzyme-catalyzed decarboxylation of OMP and FOMP provides estimates for the rate and equilibrium constants for the conformational change that traps FOMP at the enzyme active site.

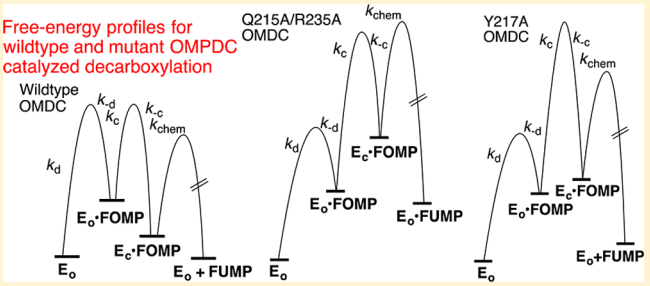

Orotidine 5′-monophosphate decarboxylase from *Saccharomyces cerevisiae* (*Sc*OMPDC) provides a large 31 kcal/mol stabilization of the transition state for decarboxylation of OMP to form uridine 5′-monophosphate [UMP (Scheme 1)],[1,2] through a UMP carbanion intermediate,[3−8] and shows an extraordinary specificity in binding this transition state with an affinity much higher than that of OMP, whose ground-state Michaelis complex is stabilized by only 8 kcal/mol.[9,10] This rate acceleration is achieved by sequestering OMP in a structured protein cage,[11−15] which provides for optimal stabilizing interactions with the decarboxylation transition state.[11,16] The protein cage is formed by an energetically demanding conformational change, driven by the binding interactions with the substrate phosphodianion and other nonreacting substrate fragments,[10,11] which function to mold two flexible protein loops into an active enzyme (Figure 1).[17]

Figure 2 shows interactions of the ligand phosphodianion with three side chains of *Sc*OMPDC: (i) the amide side chain of Gln215, (ii) the phenol side chain of Tyr217, and (iii) the guanidine side chain of Arg235.[18] The side chain of Arg235 sits on the protein surface adjacent to a phosphodianion gripper loop [Pro202−Val220 (Figure 1)]. The role of these gripper side chains was probed by preparing all combinations of single (Q215A, R235A, and Y217F), double (Q215A/Y217F, Q215A/R235A, and R235A/Y217F), and triple (Q215A/R235A/Y217F) mutants and determining the effect of these mutations on the kinetic parameters for *Sc*OMPDC-catalyzed

Received: June 1, 2015
Revised: July 1, 2015
Published: July 2, 2015

DOI: 10.1021/acs.biochem.5b00591
Biochemistry 2015, 54, 4555−4564

Scheme 1

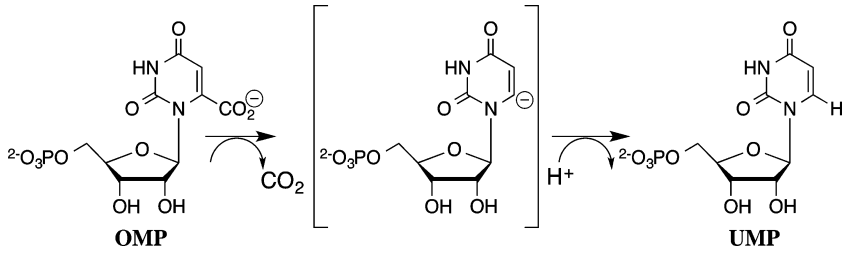

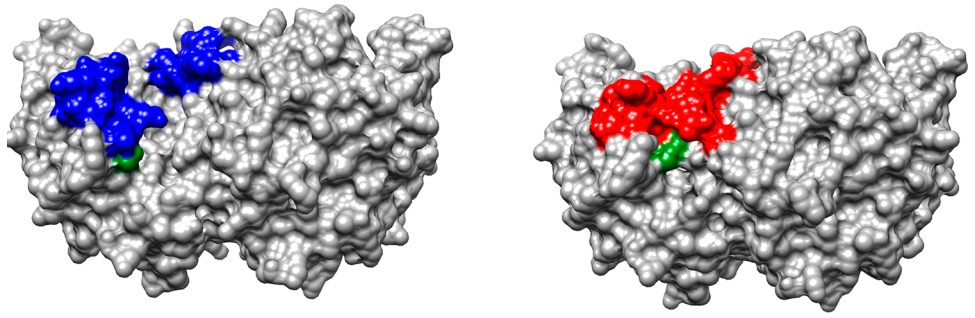

Figure 1. Space filling models of *Sc*OMPDC from yeast.[18] The structure on the left is the open unliganded form of *Sc*OMPDC (PDB entry 1DQW), and the structure on the right shows the complex with 6-hydroxyuridine 5′-monophosphate (PDB entry 1DQX). Two colored flexible loops close to form the active site cage: Pro202−Val220, on the left-hand side of each structure, interact with the substrate dianion, and Glu152−Thr165, on the right-hand side, interact with the pyrimidine ring. The guanidine side chain of R235, at the base of the left-hand loop, is colored green.

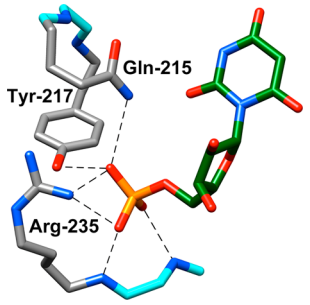

Figure 2. X-ray crystal structure (PDB entry 1DQX) of yeast *Sc*OMPDC in a complex with 6-hydroxyuridine 5′-monophosphate.[18] This structure shows the important interactions of Gln215, Tyr217, and Arg235 side chains from the phosphodianion gripper loop with the ligand phosphodianion. Reproduced from ref 4. Copyright 2012 American Chemical Society.

decarboxylation of OMP and the phosphodianion-truncated substrate 1-(β-D-erythrofuranosyl)orotic acid (EO).[4,19] The single mutations result in ≤2.5-fold decreases in k_{cat}/K_m for the catalyzed reaction of EO.[4] By contrast, these mutations result in similar large decreases in k_{cat}/K_m for *Sc*OMPDC-catalyzed decarboxylation of OMP,[19] and in the third-order rate constant for activation of *Sc*OMPDC-catalyzed decarboxylation of EO by phosphite dianion.[4] These results show that interactions of *Sc*OMPDC with the phosphodianion of OMP, or with phosphite dianion have the sole function of activating the enzyme for catalysis of decarboxylation at the distant orotate ring, through stabilization of a catalytically active caged substrate complex.[4,10,11,19] This model also provides a simple rationalization for the activation by phosphite dianion of triosephosphate isomerase[20−23] and L-glycerol 3-phosphate dehydrogenase-catalyzed reactions[24−26] of their phosphodianion-truncated substrate.

In this paper, we consider the kinetic barriers for conversion of the open form of *Sc*OMPDC to the caged complex to substrate (Figure 1), and for conversion of the caged product complex to the open enzyme. Rate constants for conformational changes that convert enzymes from an inactive to an active form may be determined directly as the appropriate

Scheme 2

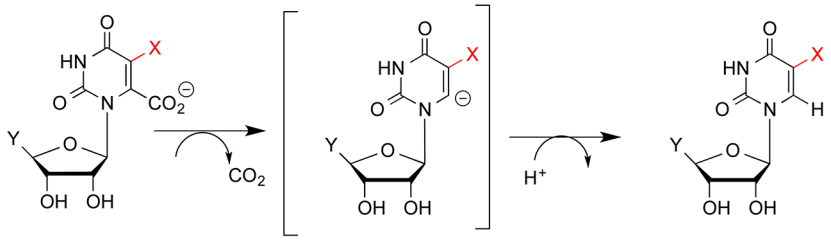

Y = -$CH_2OPO_3^{2-}$
X = H : OMP
X = F: FOMP

Y = -H
X = H : EO
X = F: FEO

DOI: 10.1021/acs.biochem.5b00591
Biochemistry 2015, 54, 4555−4564

enzyme kinetic parameter, when the conformational change is rate-determining for catalysis. Substrate binding is already partly rate-determining for *Sc*OMPDC-catalyzed decarboxylation of OMP,[9,27] while the 5-F substituent of 5-fluorouridine 5′-monophosphate (FOMP) is exceptional in providing strong stabilization of transition states for *Sc*OMPDC-catalyzed reactions.[27,28] For example, the 5-F results in a 3400-fold increase in k_{cat} for the *Sc*OMPDC-catalyzed deuterium exchange reaction of enzyme-bound UMP that proceeds through the C-6 UMP carbanion intermediate[3,6] and a 390-fold increase in the second-order rate constant k_{cat}/K_m for *Sc*OMPDC-catalyzed decarboxylation of truncated substrate EO (Scheme 2).[29,30] Now, if enzyme conformational changes are partly rate-determining for *Sc*OMPDC-catalyzed decarboxylation of OMP, then these steps should be strongly rate-determining for chemically rapid *Sc*OMPDC-catalyzed decarboxylation of FOMP.[27,28]

The 5-F at FOMP results in only small 1.1- and 6-fold increases in k_{cat}/K_m and k_{cat}, respectively, for decarboxylation of OMP (Scheme 2),[29] so that the 5-F substituent effect is only weakly expressed at the virtual transition states that govern the values of these kinetic parameters.[31] Instead, the value of k_{cat}/K_m is mainly limited by the rate of formation of the Michaelis complex, and the value of k_{cat} is mainly limited by the rate of product release.[27] The values of the kinetic parameter for decarboxylation of FOMP are not strongly affected by changes in solvent viscosity η, so that substrate binding and product release are not strictly diffusion-controlled reactions.[27] It was proposed that k_{cat}/K_m is instead limited by the rate of the protein conformational changes that follow substrate binding.[27] Roughly, a 390/1.1 = 350-fold increase (Scheme 2) in the observed rate constant of k_{cat}/K_m for decarboxylation of FOMP, relative to that for decarboxylation of OMP, is required to effect similar rate-determining decarboxylation steps for the catalyzed reactions of both OMP and FOMP.

A comparison of the effects of site-directed mutations on the kinetic parameters for *Sc*OMPDC-catalyzed decarboxylation of OMP, which is limited by chemical decarboxylation, and on *Sc*OMPDC-catalyzed decarboxylation of FOMP, which is limited by the rate of formation and breakdown of Michaelis complexes, provides insight into the effect of the mutations on the relative barriers to the chemical steps and the enzyme conformational changes.[32] We previously reported the effect of single (Q215A, R235F, and Y217F), double (Q215A/Y217F, Q215A/R235A, and R235A/Y217F), and triple (Q215A/R235A/Y217F) mutations of amino acid residues that interact with the phosphodianion of OMP (Figure 2) on the kinetic parameters for *Sc*OMPDC-catalyzed decarboxylation of OMP.[4,19] We report here the effect of these same mutations on the kinetic parameters for *Sc*OMPDC-catalyzed decarboxylation of FOMP. We note that these mutations generally cause larger changes in the values of the kinetic parameters for decarboxylation of OMP than of FOMP. This is because of their larger effects on the barrier to the decarboxylation reaction, which limits the rate of decarboxylation OMP, compared with their effect on the barrier to the enzyme conformational change, which limits the rate of decarboxylation of FOMP.[27] We also note interesting exceptions to this trend, which show that mutations of gripper side chains cause significant changes in the barriers to the protein conformational changes, which control the rate constants for formation and breakdown of complexes between *Sc*OMPDC and FOMP or FUMP.

EXPERIMENTAL PROCEDURES

Materials. OMP[28,29] and FOMP[29,33] were prepared enzymatically by literature procedures. 3-(*N*-Morpholino)-propanesulfonic acid (MOPS, ≥99.5%) was purchased from Fluka. All other chemicals were reagent grade or better and were used without further purification.

Wild-Type and Mutant Forms of *Sc*OMPDC. Plasmid pScODC-15b containing the gene encoding *Sc*OMPDC from *S. cerevisiae* with an N-terminal His_6 or His_{10} tag was available from previous studies.[27,34] The procedures for the preparation of the Q215A,[34] Y217F,[4] Y217A,[5] Q215A/Y217F,[4] Q215A/R235A,[4] Y217F/R235A,[4] Q215A/Y217F/R235A,[4] S154A,[34] and Q215A/S154A[34] mutant enzymes were described in earlier work. In all cases, the N-terminal His_6 or His_{10} tag was removed by the action of thrombin (1 unit/mg of mutant *Sc*OMPDC) at room temperature for ∼16 h, as described in the Supporting Information of ref 34. Wild-type and mutant forms of *Sc*OMPDC were stored at −80 °C. Prior to use, frozen *Sc*OMPDC was defrosted and dialyzed at 4 °C against 10 mM MOPS (50% free base) and 100 mM NaCl (pH 7.1).

Kinetic Parameters for Decarboxylation of FOMP. The following conditions were used for all enzyme assays: 30 mM MOPS (50% free base) at pH 7.1 (30 mM MOPS), 25 °C, and I = 0.105 (NaCl). The concentration of *Sc*OMPDC in stock enzyme solutions was determined from the absorbance at 280 nm using values of 29900 M^{-1} cm^{-1} for wild-type and most mutant enzymes or 28400 M^{-1} cm^{-1} for the Y217F and Y217A mutants that were calculated using the ProtParam tool available on the ExPASy server.[35,36] Initial velocities, v_0 (M s^{-1}), for decarboxylation of FOMP (0.01−3.0 mM) catalyzed by mutants of yeast *Sc*OMPDC were determined spectrophotometrically by following the decrease in absorbance at 282, 290, 295, or 300 nm. The following values for the difference in the extinction coefficient of FOMP and FUMP were determined from the initial absorbance of a solution that contains a known concentration of FOMP, and the final absorbance after quantitative enzyme-catalyzed decarboxylation to form FUMP: −1380, −1090, −805, and −490 M^{-1} cm^{-1} for FOMP at 282, 290, 295, and 300 nm, respectively. The following wavelengths were generally monitored for enzyme-catalyzed decarboxylation reactions at different [FOMP]: [FOMP] ≤ 0.2 mM at 282 nm, [FOMP] = 0.2−0.4 mM at 290 nm, [FOMP] = 0.3−0.8 mM at 295 nm, and [OMP] ≥ 0.8 mM at 300 nm. Enzyme-catalyzed decarboxylation of FOMP, in a total volume of 1 mL, was initiated by the addition of 1−10 μL of a stock solution of mutant *Sc*OMPDC to give the following enzyme concentrations: 5−10 nM, Q215A and Y217F mutants; 200 nM, Q215A/R235A mutant; 1.8 μM, Y217F/R235A mutant; 50−100 nM, S154A and S154A/Q215A mutants; 200 nM, Y217A mutant. Initial reaction velocity v_0 was determined for the decarboxylation of the first ∼5% of FOMP. Values of k_{cat} and K_m for the mutant enzyme-catalyzed reactions were obtained from the nonlinear least-squares fits of the values of $v_0/[E]$ (s^{-1}) to the Michaelis−Menten equation.

The decarboxylation of FOMP (50 μM) catalyzed by the Q215A/Y217F/R235A triple mutant of *Sc*OMPDC was monitored over 8−10 reaction half times. Reactions in a volume of 1 mL were initiated by addition of 100 μL of a stock solution of the mutant enzyme to give a final concentration of 25 μM and then monitored spectrophotometrically at 295 nm. The rate constants k_{obs} (s^{-1}) for first-order decay of FOMP to

DOI: 10.1021/acs.biochem.5b00591
Biochemistry 2015, 54, 4555−4564

FUMP were obtained by fitting the absorbance date to the equation for an exponential decay. The value of k_{cat}/K_m ($M^{-1}s^{-1}$) was then calculated from the relationship $k_{cat}/K_m = k_{obsd}/[E]$.

RESULTS

Panels A–C of Figure 3 show the fits of plots of $v_0/[E]$ versus [FOMP] to the Michaelis–Menten equation for decarboxylation of FOMP catalyzed by site-directed mutants of *Sc*OMPDC in solutions that contain 30 mM MOPS (50% free base) at pH 7.1, 25 °C, and I = 0.105 (NaCl). These fits gave the values for k_{cat} and K_m for the mutant enzyme decarboxylation of FOMP reported in Table 1, with the exception of data for the reaction catalyzed by the Y217F/R235A mutant, which were fit to a linear equation to give the value for k_{cat}/K_m. The value of k_{cat}/K_m for the Q215A/Y217F/R235A triple mutant *Sc*OMPDC-catalyzed reaction was determined by monitoring the entire time course for the decarboxylation of 50 μM FOMP ($K_m \gg 50$ μM) as described in Experimental Procedures. Table 1 reports the kinetic parameters k_{cat}, K_m, and k_{cat}/K_m for wild-type and mutant *Sc*OMPDC-catalyzed decarboxylation of FOMP determined in this study. The corresponding kinetic parameters for decarboxylation of OMP were reported previously.[19,34,37] We note a k_{cat} of 4.7 s^{-1}, a K_m of 0.0019 M^{-1}, and a k_{cat}/K_m of 2500 M^{-1} s^{-1} reported for decarboxylation of OMP catalyzed by the Y217A mutant of *Sc*OMPDC in solutions that contain 30 mM MOPS (50% free base) at pH 7.1, 25 °C, and I = 0.105 (NaCl).[37] By comparison, a k_{cat} of 2.0 s^{-1}, a K_m of 9.4 × 10^{-5} M^{-1}, and a k_{cat}/K_m of 21000 M^{-1} s^{-1} were reported for the reaction catalyzed by this mutant at an undefined low ionic strength.[38] A decrease in ionic strength from I = 0.105 to I = 0.020 was shown in earlier work to result in a 9-fold decrease in K_m and k_{cat}/K_m for the decarboxylation of OMP catalyzed by the R235A mutant of *Sc*OMPDC.[29]

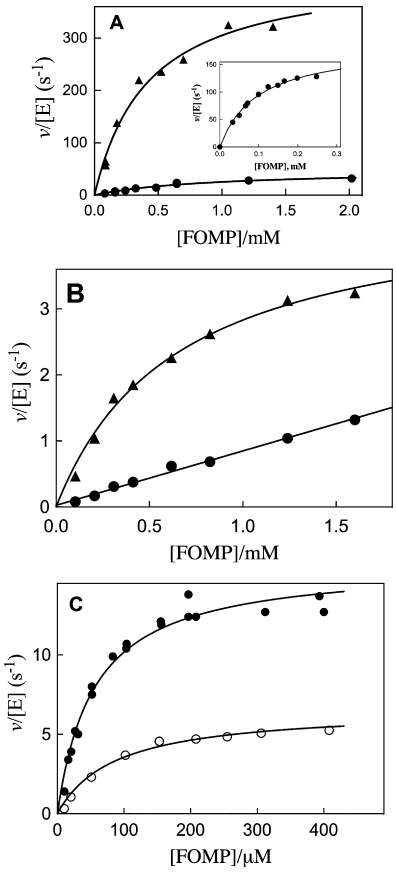

Figure 3. Dependence of $v/[E]$ for decarboxylation of FOMP catalyzed by mutant forms of *Sc*OMPDC on the concentration of FOMP for reactions at 25 °C, pH 7.1 (30 mM MOPS), and I = 0.105 (NaCl): (A) (▲) Y217F mutant, (●) Q215A/Y217F mutant, and (inset) Q215A mutant; (B) (▲) Q215A/R235A mutant and (●) Y217F/R235A mutant; and (C) (●) S154A mutant and (○) Q215A/S154A mutant.

DISCUSSION

An enzyme conformational change at the ternary E·FEO·HPO_3^{2-} complex is rate-determining for phosphite dianion activation of *Sc*OMPDC-catalyzed decarboxylation of the fluorinated–truncated substrate FEO to form FEU.[30] The 1.1-fold effect of the 5-F at the whole substrate FOMP on k_{cat}/K_m for wild-type *Sc*OMPDC-catalyzed decarboxylation of OMP shows that there is minimal stabilization of this rate-determining transition state by polar/electrostatic interactions between the electronegative -F and transition-state negative charge at C-6. The simplest interpretation is that k_{cat}/K_m is limited by the rate of diffusion-controlled formation of the Michaelis complex between *Sc*OMPDC and FOMP. However, a study of the effect of changes in solvent viscosity (η_o) on kinetic parameter $(k_{cat}/K_m)_o$ for decarboxylation in water gave slopes of 0.37 and 0.64 for plots of $(k_{cat}/K_m)_o/(k_{cat}/K_m)_{obs}$ for decarboxylation of OMP and FOMP, respectively, against η/η_o,[27] which are smaller than the slope of 1.0 expected for a diffusion-limited reaction.[39] This shows that the rate of formation of the Michaelis complex is partly limited by a second step, which we propose is the conformational change that traps FOMP in a protein cage [k_c (Scheme 3)].[27]

The small value of $(k_{cat})_F/(k_{cat})_H$ = 6 for *Sc*OMPDC-catalyzed decarboxylation of OMP and FOMP, compared to ratios observed when the entire 5-F substituent effect on carbanion stability is expressed at the rate-determining transition state (Scheme 2), shows that decarboxylation of FOMP is not limited by rate constant k_{chem} (Scheme 3) for decarboxylation of bound substrate. Slopes of 0.39 and 1.0, respectively, were determined for plots of $(k_{cat})_{obs}/(k_{cat})_o$ for decarboxylation of OMP and FOMP, respectively, versus η/η_o.[27] These are consistent with the conclusion that k'_{-c} and/or k'_{-d} are partly rate-determining for *Sc*OMPDC-catalyzed decarboxylation of OMP (Scheme 3) and fully rate-determining for decarboxylation of FOMP.

Simple Conclusions about the Effect of Mutations on 5-F Substituent Effects. The effect of the 5-F at FOMP on the kinetic parameters k_{cat}/K_m and k_{cat} for *Sc*OMPDC-catalyzed decarboxylation of OMP, when chemical decarboxylation is clearly rate-determining, should be similar to the 390-fold effect of 5-F on k_{cat}/K_m for *Sc*OMPDC-catalyzed decarboxylation of the phosphodianion-truncated substrate EO (Scheme 2). Table 1 shows that the values of $(k_{cat}/K_m)_F/(k_{cat}/K_m)_H$ increase as *Sc*OMPDC is crippled by mutations of gripper side chains to 760 for the Q215A/Y217A/R235A triple mutant, consistent with rate-determining decarboxylation for the two substrates. The largest observed ratio of $(k_{cat})_F/(k_{cat})_H$ is 240 for the Q215A/R235A mutant enzyme-catalyzed reactions. The more severely crippled mutants bind OMP and FOMP too weakly to approach saturation.

DOI: 10.1021/acs.biochem.5b00591
Biochemistry 2015, 54, 4555–4564

Table 1. Effect of Mutations of Phosphodianion Gripper Amino Acid Residues on the Kinetic Parameters for *Sc*OMPDC-Catalyzed Decarboxylation of FOMP[a]

*Sc*OMPDC	k_{cat} (s^{-1})[b]	$(k_{cat})_F/(k_{cat})_H$[h]	K_m (M)[b]	k_{cat}/K_m (M^{-1} s^{-1})	$(k_{cat}/K_m)_F/(k_{cat}/K_m)_H$[h]
wild-type[c]	95	6	8×10^{-6}	1.2×10^{7}	1.1
Q215A[d]	190 ± 10	8	$(9.6 \pm 1) \times 10^{-5}$	2.0×10^{6}	8
Y217F[d]	430 ± 30	21	$(4.2 \pm 0.6) \times 10^{-4}$	1.1×10^{6}	6
R235[c]	92	92	5.8×10^{-4}	1.6×10^{5}	180
Q215A/Y217F[d]	49 ± 5	10	$(9.2 \pm 1.7) \times 10^{-4}$	5.3×10^{4}	16
Q215A/R235A[e]	4.7 ± 0.3	240	$(6.5 \pm 0.8) \times 10^{-4}$	7200	500
Y217F/R235A[e]				820	200
triple mutant				28	760
S154A[f]	16 ± 0.5	200[i]	$(5.5 \pm 0.6) \times 10^{-5}$	2.9×10^{5}	460[i]
S154A/Q215A[f]	6.6 ± 0.3	160[i]	$(8.6 \pm 1.3) \times 10^{-5}$	7.7×10^{4}	200[i]
Y217A[g]	8.2 ± 0.5	2[g]	$(6.2 \pm 0.6) \times 10^{-4}$	1.3×10^{4}	5[g]

[a]For reactions at pH 7.1 (30 mM MOPS), 25 °C, and I = 0.105 (NaCl). [b]The quoted errors are the standard deviations obtained from the nonlinear least-squares fits of data from panels A–C of Figure 3 to the Michaelis–Menten equation. [c]From ref 29. [d]Figure 3A. [e]Figure 3B. [f]Figure 3C. [g]Kinetic parameters for reactions of OMP from ref 37. [h]Kinetic parameters for reactions of OMP from ref 19, unless indicated otherwise. [i]Kinetic parameters for reactions of OMP from ref 34.

Scheme 3

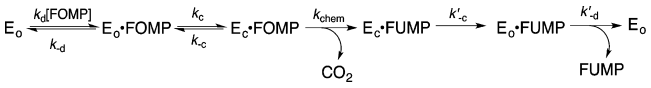

Single mutations of gripper side chains result in increases in k_F/k_H for kinetic parameters k_{cat} and k_{cat}/K_m, because of the stronger effect of the mutations on k_{cat} and k_{cat}/K_m for enzyme-catalyzed decarboxylation of OMP. The following effects of Q215A and Y217F single mutations on k_F/k_H for kinetic parameters k_{cat}/K_m and k_{cat} provide strong evidence that the mutations affect the rate constants for binding and release of FOMP.

(1) The Q215A and Y217F mutations of *Sc*OMPDC cause $(k_{cat}/K_m)_F/(k_{cat}/K_m)_H$ to increase to 8 and 6, respectively. These are still much smaller than the ratio of ≈400 for rate-determining decarboxylation. Therefore, formation of the E_C·FOMP complex remains rate-determining for the mutant enzyme-catalyzed reactions. The mutations result in surprising 6- and 10-fold decreases in k_{cat}/K_m for Q215A and Y217F mutant enzyme-catalyzed decarboxylation of FOMP, respectively (Table 1), which can reflect only decreases in k_c for rate-determining conversion of E_O·FOMP to E_C·FOMP (Scheme 3). This shows that a weakening of the protein–phosphodianion interactions by these mutations results in a decrease in the rate of enzyme conformational change, which allows expression of these interactions (Figure 2).

(2) The Q215A and Y217F mutations of *Sc*OMPDC cause an increase in $(k_{cat})_F/(k_{cat})_H$, which is due mainly to a surprising increase in $(k_{cat})_F$ for decarboxylation of FOMP by rate-determining breakdown of E_C·FUMP (Scheme 3). We conclude that $k_{cat} \approx k'_{-c} = 95$ s^{-1} (Scheme 3) for the wild-type enzyme-catalyzed reaction and that weakening of the protein–dianion interactions results in an increase in k'_{-c} (Scheme 3) for the rate-determining enzyme conformational change.

The S154A mutation results in large 180- and 15000-fold decreases in kinetic parameters k_{cat} and (k_{cat}/K_m), respectively, for decarboxylation of OMP[34] but much smaller 6- and 41-fold decreases in k_{cat} and (k_{cat}/K_m), respectively, for decarboxylation of FOMP (Table 1). Consequently, the S154A mutant shows a high reactivity toward catalysis of decarboxylation of FOMP: $(k_{cat}/K_m)_F/(k_{cat}/K_m)_H = 460$, and $(k_{cat})_F/(k_{cat})_H = 200$. These 5-F effects are similar to the 400-fold effect of the 5-F on k_{cat}/K_m for decarboxylation of the phosphodianion-truncated substrate EO (Scheme 2). We conclude that the stabilizing interactions between the 5-F and neighboring C-6 carbanion are strongly expressed at the rate-determining transition state for decarboxylation of FOMP catalyzed by S154A mutant *Sc*OMPDC. We suggest that the ∼2-fold larger 5-F substituent effect on k_{cat}/K_m compared with that on k_{cat} reflects the small stabilization of the Michaelis complex to FOMP by an interaction between the protein and the 5-F substituent.

The CH_2OH side chain of Ser154 accepts a hydrogen bond from the pyrimidine NH group and acts as a hydrogen bond donor to the oxygen of the amide side chain of Gln215 (Figure 4).[18,34] The second H-bond acts to clamp two enzyme loops over the pyrimidine ring and the phosphodianion of OMP. The effect of these individual mutations on the kinetic parameters for decarboxylation of OMP depends upon the order of the amino acid substitutions.[34] The 6 kcal/mol total side chain

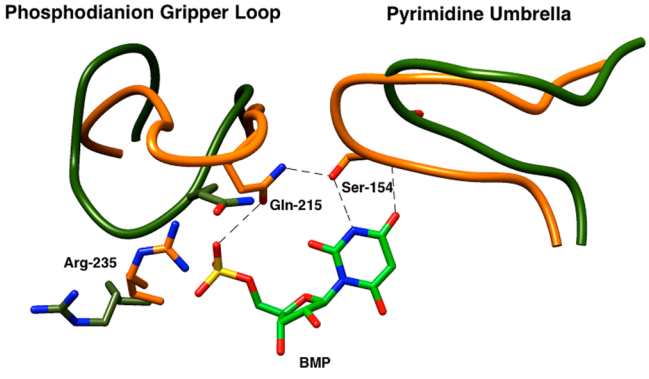

Figure 4. Partial X-ray crystal structure of *Sc*OMPDC complexed with 6-hydroxyuridine 5′-monophosphate (PDB entry 1DQX) superimposed over the structure for unliganded *Sc*OMPDC (PDB entry 1DQW). The movement of the phosphodianion gripper loop (Pro202–Val220) toward the hydrophobic pyrimidine umbrella (Glu152–Thr165) is shown for the unliganded (olive green) and liganded (orange) enzymes. The closure of these loops is cooperative and driven by the formation of a hydrogen bond between the side chains of Gln215 from the "gripper" loop and of Ser 154 from the "umbrella". Reproduced from ref 29. Copyright 2013 American Chemical Society.

DOI: 10.1021/acs.biochem.5b00591
Biochemistry 2015, 54, 4555–4564

interactions can be partitioned into an ~2 kcal/mol interaction between the amide side chain of Gln215 and the phosphodianion group of OMP, observed for the Q215A mutation of wild-type *Sc*OMPDC, and an ~4 kcal/mol interaction between the -CH_2OH side chain of Ser154 and the pyrimidine ring of OMP, observed for the S154A mutation of Q215A mutant *Sc*OMPDC. The opposite order of these mutations leads to expression of nearly the entire 6 kcal/mol effect observed for the S154A/Q215A double mutation at the S154A single mutant, with only a small 0.3 kcal/mol additional effect of the second Q215A mutation.[34] These results reflect cooperativity in the interactions of these side chains with the transition state for decarboxylation, due to the requirement for a hydrogen bond between the -CH_2OH group of Ser154 and the amide side chain of Gln215 to position the latter side chain to interact with the phosphodianion group of OMP. It was proposed that the S154A single mutation leads to loss of the transition-state stabilization contributed by the side chains of both Ser154 and Gln215. These trends are hardly discernible in the effects of the same mutations on the kinetic parameters for *Sc*OMPDC-catalyzed decarboxylation of FOMP, because the large effects on the rate of chemical decarboxylation are weakly expressed as changes in the enzyme kinetic parameters.

Eliminating Protein−Phosphodianion Interactions. The results from a recent study on the effect of mutations of gripper side chains on the kinetic parameters for *Sc*OMPDC-catalyzed decarboxylation of EO and OMP provide strong evidence that the effects of these mutations on the enzyme kinetic parameters for decarboxylation of OMP are due essentially entirely to changes in the relative stability of the inactive open and active closed forms of *Sc*OMPDC (Scheme 4).[4,19,29] We will summarize the experimental evidence that supports the model shown in Scheme 4[4,19,29] and then use this model in the interpretation of the effects of these mutations on the kinetic parameters for *Sc*OMPDC-catalyzed decarboxylation of FOMP.

Scheme 4

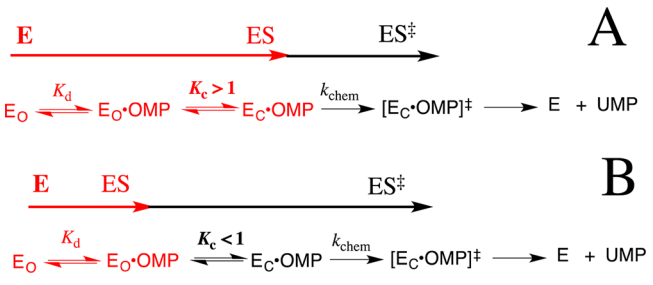

(1) The Q215A, Y217A, and R235A single mutations result in ≥2.5-fold decreases in k_{cat}/K_m for decarboxylation of the phosphodianion-truncated substrate EO,[4] but in much larger decreases in the third-order rate constant for phosphite dianion activation of *Sc*OMPDC-catalyzed decarboxylation of EO,[4] and in the second-order rate constant k_{cat}/K_m for decarboxylation of OMP.[19] The first result shows that there is little or no direct interaction between the loop side chains and the site of chemical decarboxylation of the orotate ring. It was concluded that the large effect of these mutations on the kinetic parameters for dianion activation of decarboxylation of EO and for decarboxylation of OMP is entirely due to the loss of stabilizing interactions between the deleted side chains and the enzyme-bound dianion.[4,19]

(2) The model in Scheme 4 was used to rationalize the effects of mutations of gripper side chains on the kinetic parameters for *Sc*OMPDC-catalyzed decarboxylation of OMP. The complex between wild-type *Sc*OMPDC and OMP is proposed to exist mainly in the closed form [$K_c \gg 1$ (Scheme 4A)]. Consequently, the first mutations of gripper side chains, which result in up to 4 kcal/mol destabilization of E_C, are entirely expressed as a decrease in the Michaelis constant to the limiting value of $(K_m)_{obs} = K_d = 1$ mM for dissociation of OMP from E_O·OMP. Mutations that result in further decreases to K_c values of <1 then lead to a decrease in k_{cat}, which falls below the invariant value of k_{chem} for *Sc*OMPDC-catalyzed decarboxylation of OMP (Scheme 3).[19] This is because the loop dianion interactions now only develop on proceeding from the dominant Michaelis complex (E_O·OMP) to the transition state for decarboxylation at E_C·OMP [$ES^‡$ (Scheme 4B)]. We estimate a K_c value of ≈1000 (Table 2) for the reaction catalyzed by wild-type *Sc*OMPDC from the difference in $K_d = 1$ μM for decarboxylation of OMP[9] and estimated $K_d \approx 1$ mM for dissociation of OMP from E_O·OMP.[19]

Microscopic Rate Constants. *Wild-Type ScOMPDC.* Substrate binding (k_d) and enzyme conformational change k_c are each partly rate-determining for wild-type *Sc*OMPDC-catalyzed decarboxylation of FOMP at [FOMP] ≪ K_m, so that $k_{-d} \approx k_c$ (Scheme 5).[27] Combining the values of $(k_{cat}/K_m) \approx k_d = 1.2 \times 10^7$ M^{-1} s^{-1} for encounter-limited decarboxylation of FOMP determined for wild-type OMPDC and $K_d = (k_{-d}/k_d) \approx 10^{-3}$ M [1 mM (see above)] for breakdown of the E_O·FOMP

Table 2. Microscopic Rate Constants for Decarboxylation of FOMP (Scheme 5) by Wild-Type and Mutant Forms of *Sc*OMPDC at pH 7.1 (30 mM MOPS), 25 °C, and *I* = 0.105 (NaCl), Calculated As Described in the Text

*Sc*OMPDC	k_{cat} (s^{-1})[a]	k_{chem} (s^{-1})[b]	$[(k_{cat})_{wt}/(k_{cat})_{mut}]_{OMP}$[c]	K_c[d]	k_c (s^{-1})[e]	k_{-c} (s^{-1})[f]	Λ[g] (kcal/mol)	k_0 (s^{-1})[h]
wild-type	95	5000		1000	10^4	10	13.9	350
R235A	92	5000	15	0.071	120	1800	13.7	500
Q215A/R235A	4.7	5000	750	0.0013	17	13000	13.7	560
Q215A/Y217F	49	5000	3.1	0.48	50	100	14.9	70
Y217A	8.2	5000	3.2	0.45	8.2	18	15.9	12

[a]Table 1. [b]Calculated from $k_{cat} = 15$ s^{-1} for decarboxylation of OMP[19] and the ratios $k_{chem}/k_{cat} = 1.8$ for decarboxylation of OMP,[9] where k_{cat} is the true decarboxylation rate constant, and $(k_{cat})_F/(k_{cat})_H \approx 200$ (Table 1) when chemistry is rate-determining for *Sc*OMPDC-catalyzed decarboxylation of OMP and FOMP (Table 1). [c]The ratio of observed rate constants k_{cat} for decarboxylation of OMP catalyzed by wild-type [$(k_{cat})_{wt}$] and mutant [$(k_{cat})_{mut}$] forms of *Sc*OMPDC.[19] [d]Estimated equilibrium constants for conversion of E_O·OMP to E_C·OMP (Scheme 5), calculated for mutants of *Sc*OMPDC using eq 1. [e]Rate constant for conversion of E_O·OMP to E_C·OMP, calculated using eqs 2 and 3. [f]Rate constant for conversion of E_C·OMP to E_O·OMP. [g]Marcus intrinsic reaction barrier, calculated using eq 5. [h]Rate constant for a hypothetical thermoneutral reaction calculated using eq 6.

DOI: 10.1021/acs.biochem.5b00591
Biochemistry 2015, 54, 4555−4564

Scheme 5

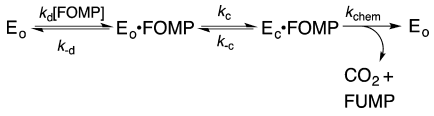

complex gives $k_c \approx k_{-d} = 10^4\ s^{-1}$ for the enzyme conformational change (Table 2). The value of $k_{chem} = 5000\ s^{-1}$ for decarboxylation at E_C·FOMP by wild-type *Sc*OMPDC (Table 2) was calculated from $k_{cat} = 15\ s^{-1}$ for decarboxylation of OMP,[19] and the ratios $k_{chem}/k_{cat} = 1.8$ for decarboxylation of OMP,[9] where k_{chem} is the true decarboxylation rate constant, and $(k_{cat})_F/(k_{cat})_H \approx 200$ when chemistry (Table 1) is rate-determining for OMPDC-catalyzed reactions of both substrates.

Mutants of ScOMPDC. The Q215A and Y217F mutations each cause k_{cat} for turnover of FOMP to increase above the value of $k_{cat} = 95\ s^{-1}$ for wild-type *Sc*OMPDC, because of an increase in the rate of release of product to water (Table 1). By contrast, the more severe R235A, Q215A/Y217F, and Q215A/R235A mutations cause k_{cat} to decrease to a value as small as $4.7\ s^{-1}$ for the Q215A/R235A mutant (Table 1). The value of k_{chem} for the reaction of E_C·FOMP is not affected by mutations of the gripper residues, because there are only weak interactions between these side chains and the orotate ring at the transition state for *Sc*OMPDC-catalyzed decarboxylation of enzyme-bound substrate.[4,19] Rather, the decreases in k_{cat}, as the protein dianion interactions are weakened and product release becomes much faster than turnover, show that the values of rate constants k_c, k_{-c}, and k_{chem} (Scheme 5, which omits the step for product release) begin to control the observed value of k_{cat}.

Equation 1 relates the equilibrium constant K_c for loop closure at mutant *Sc*OMPDCs to the effect of the individual mutation on $(k_{cat})_{wt}$ for wild-type *Sc*OMPDC-catalyzed decarboxylation of OMP. This equation was derived by assuming that these mutations do not affect microscopic rate constant k_{chem} for decarboxylation of E_C·OMP, and that the entire decrease in $(k_{cat})_{mut}$ compared to $(k_{cat})_{wt}$ is due to the decrease, from the value of $f_{EC} = 1.0$ for wild-type *Sc*OMPDC, in the fraction of the Michaelis complex present in the reactive E_C·OMP form during turnover $[(k_{cat})_{mut} = (k_{cat})_{wt} f_{EC}]$. The estimated values of K_c reported in Table 2 for mutant *Sc*OMPDC-catalyzed decarboxylation of FOMP were calculated using eq 1 (Scheme 3), and assuming identical values of K_c for loop closure over OMP and FOMP.

$$1/(K_c)_{mut} = \frac{(k_{cat})_{wt}}{(k_{cat})_{mut}} - 1 \quad (1)$$

Table 2 reports estimated rate constants (Scheme 5) for mutants of *Sc*OMPDC, which were calculated from $k_{chem} = 5000\ s^{-1}$, the values of $(k_{cat})_{mut}$ for decarboxylation of FOMP (Table 1) and of K_c for the enzyme conformational change (see above), and using eqs 2 and 3 derived for Scheme 5. We note again this treatment assumes that mutations of gripper side chains do not affect the value of k_{chem} (Scheme 5) for decarboxylation of OMP and FOMP. The observation that this treatment provides a rationalization for the following otherwise confusing effects of the mutations of gripper side chains on the kinetic parameters for decarboxylation of OMP and FOMP provides strong justification for the simplifying assumptions used in the calculation of the rate constants from Table 2.

$$(k_{cat})_{mut} = \frac{k_c k_{chem}}{k_{-c} + k_{chem}} \quad (2)$$

$$K_c = \frac{k_c}{k_{-c}} \quad (3)$$

(1) The 5-fold larger value of k_{cat} for decarboxylation of OMP catalyzed by the Q215A/Y217F mutant ($4.8\ s^{-1}$) compared with that for the R235A mutant ($1.0\ s^{-1}$) is due to the larger effect of the R235A mutation on the equilibrium constant K_c (Table 2).[19] By contrast, the Q215A/Y217F mutant shows a 2-fold smaller value of k_{cat} for decarboxylation of FOMP (Table 1). We propose that the k_{cat} values of 49 and $92\ s^{-1}$ for the Q215A/Y217F and R235A mutant *Sc*OMPDC-catalyzed decarboxylations of FOMP, respectively, are limited by the k_c values of 50 and $120\ s^{-1}$ for loop closure to form E_C·FOMP (Table 2). In other words, rate-determining loop closure during R235A mutant enzyme-catalyzed decarboxylation of FOMP is faster than for the Q215A/Y217F mutant enzyme-catalyzed reaction, in spite of the 5-fold more unfavorable equilibrium constant for loop closure at the R235A mutant.

(2) The large value of $(k_{cat})_F/(k_{cat})_H = 240$ for decarboxylation catalyzed by Q215A/R235A mutant *Sc*OMPDC shows that the step for k_{chem} for decarboxylation of E_C·FOMP limits the value of k_{cat} for turnover (Scheme 3). The k_{cat} value of $4.7\ s^{-1}$ for decarboxylation of FOMP catalyzed by this mutant is much smaller than the k_{chem} of $\approx 5000\ s^{-1}$ and the k_c of $=17\ s^{-1}$ (Table 2), because the barrier to decarboxylation k_{cat} includes the ~4 kcal/mol barrier for conversion of E_O·FOMP to E_C·FOMP [$K_c = 1/750$, and $k_{-c} = 13000\ s^{-1}$ (Table 2)]. In other words, loop closure over enzyme-bound FOMP is partly reversible ($k_{-c} > k_{chem}$) so that decarboxylation at E_C·FOMP (k_{chem}) is the rate-determining step.

(3) The Y217A mutation results in similar large decreases in k_{cat} and k_{cat}/K_m for wild-type *Sc*OMPDC-catalyzed decarboxylation of both OMP and FOMP, so that there is only a small effect of the 5-F substituent on the kinetic parameters for this mutant enzyme-catalyzed reaction: $(k_{cat})_F/(k_{cat})_H = 2$, and $(k_{cat}/K_m)_F/(k_{cat}/K_m)_H = 5$ (Table 1). We conclude that the Y217A mutation results in a similar increase in the barriers to decarboxylation of OMP, where chemistry is rate-determining, and for decarboxylation of FOMP, where the enzyme conformational change is rate-determining. This is reflected by the large decrease in rate constant k_c for the enzyme conformational change (Scheme 5) to form the loop-closed *Sc*OMPDC (Table 2).

$$\frac{k_{cat}}{K_m} = \left(\frac{1}{K_d}\right)\left(\frac{k_c k_{chem}}{k_{-c} + k_{chem}}\right) \quad (4)$$

(4) Equations 2 and 4 are derived for mutants (Table 2) whose reaction is described by Scheme 5. These equations predict that kinetic parameters k_{cat} and k_{cat}/K_m for decarboxylation of FOMP are related by $1/K_d$ for formation of E_O·FOMP. This provides a rationalization for the observation that the kinetic data from Table 1 can be used to calculate a nearly constant ratio of $k_{cat}/(k_{cat}/K_m) \approx K_d = 6\text{–}9 \times 10^{-4}$ M for decarboxylation of FOMP catalyzed by the different mutants from Table 2, which is similar to $K_d \approx 10^{-3}$ M estimated in earlier work for the release of substrate from E_O·OMP to form E_O.[19]

DOI: 10.1021/acs.biochem.5b00591
Biochemistry 2015, 54, 4555–4564

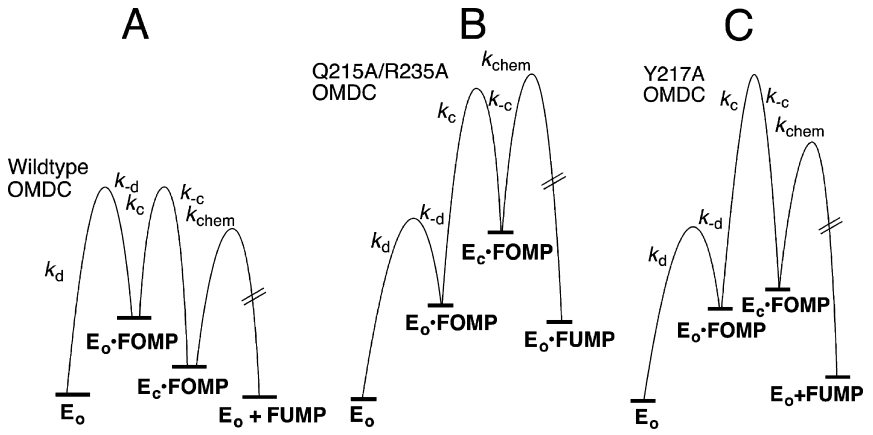

Figure 5. Free energy profiles for *Sc*OMPDC-catalyzed decarboxylation of FOMP (Scheme 5), drawn for reactions at $[S] \ll K_m$ using the kinetic parameters from Table 2. (A) Decarboxylation of FOMP catalyzed by wild-type OMPDC, which shows (a) the similar barriers to partitioning of E_O·FOMP between dissociation of OMP and the enzyme conformational change to form E_C·FOMP ($k_{-d} \approx k_c$),[27] (b) thermodynamically favorable conversion of E_O·FOMP to the E_C·FOMP caged complex,[19] and (c) the ≈3.5 kcal/mol difference [RT ln(390/1.1) (Scheme 2)] between the barriers for formation of E_C·FOMP and decarboxylation of E_C·FOMP. (B) Decarboxylation of FOMP catalyzed by the Q215A/R235A mutant of *Sc*OMPDC. This mutation results in a 10^6-fold decrease in K_c for loop closure compared with that of wild-type *Sc*OMPDC, but in little change in intrinsic barrier Λ for loop closure (Table 2). The decarboxylation step is rate-determining because $k_{-c} > k_{chem}$. (C) Decarboxylation of FOMP catalyzed by the Y217A mutant of *Sc*OMPDC. This mutation results in a 2000-fold decrease in K_c for loop closure and a large increase in intrinsic barrier Λ for slow loop closure (Table 2), so that loop closure is rate-determining for this decarboxylation reaction.

Free Energy Reaction Profiles. Figure 5 shows free energy profiles for *Sc*OMPDC-catalyzed decarboxylation of FOMP catalyzed by wild-type OMPDC (Figure 5A), the Q215A/R235A (Figure 5B), and Y217A (Figure 5C) mutant enzymes, drawn using the kinetic parameters from Table 2 for reactions at $[S] \ll K_m$. These profiles rationalize the two very different effects of the 5-F substituent on mutant-enzyme catalyzed decarboxylation of OMP.

(1) The large 240- and 500-fold 5-F substituent effects on k_{cat} and k_{cat}/K_m for Q215A/R235A *Sc*OMPDC-catalyzed decarboxylation show that the step for chemical decarboxylation, k_{chem} (Scheme 5), limits the values of these kinetic parameters. This reflects the small barrier to k_{-c} for fast loop opening at the crippled enzyme, relative to the barrier for k_{chem} for decarboxylation, which is not affected by these mutations. Figure 5B shows that the overall barrier to k_{cat}/K_m is the sum of the barriers to (i) formation of the Michaelis complex ($[S] \ll K_m$), (ii) K_c for the enzyme conformational change, and (iii) the activation barrier to k_{chem}.

(2) By comparison, the small 2- and 5-fold effects of 5-F on k_{cat} and k_{cat}/K_m for Y217A mutant *Sc*OMPDC-catalyzed decarboxylation of OMP (Table 2) show that a slow enzyme conformational change is rate-determining for the mutant enzyme-catalyzed decarboxylation reaction (Figure 5C). Now, the expected increase in k_{-c} for loop opening for the mutant enzyme, due to the effect of the mutation on K_c (Table 2), has been approximately balanced by a second effect of this mutation that results in a decrease in k_{-c}.

Intrinsic Reaction Barriers. Similar rate constants (k_c) are estimated for the Q215A/R235A [100 s^{-1} (Table 2)] and Y217A (18 s^{-1}) mutant enzyme-catalyzed reactions; however, the conformational change for the Q215A/R235A mutant is relatively slow because of the large unfavorable thermodynamic driving force ($K_C = 1.3 \times 10^{-3}$), while this conformational change for the Y217A mutant is slow because of the large intrinsic kinetic reaction barrier. These intrinsic kinetic barriers Λ (kilocalories per mole) may be defined by the Marcus equation (eq 5) as the reaction barrier in the absence of a thermodynamic driving force ($\Delta G^\circ = 0$).[40−45] Intrinsic barriers Λ for loop closure, with different *Sc*OMPDC mutants, were estimated from rate constants k_c and corresponding equilibrium constants K_c reported in Table 2, using eq 5, derived for a reaction at 298 K.[46,47] The Marcus intrinsic rate constants for hypothetical thermoneutral loop closure reactions at the different mutant enzymes (Table 2) were then estimated from Λ using eq 6, also derived at 298 K.[46,47]

$$\log k_c = \frac{1}{1.36}\left[17.44 - \Lambda\left(1 - \frac{1.36 \log K_c}{4\Lambda}\right)^2\right] \quad (5)$$

$$\log k_o = 12.8 - \frac{\Lambda}{1.36} \quad (6)$$

Table 2 shows that the R235A/Q215A double mutation results in an ≈10^6-fold decrease in K_c for loop closure but causes little change in intrinsic barrier Λ for the enzyme conformational change. By contrast, the Q215A/Y217F double mutation results in a 1.2 kcal/mol increase in Λ, which we attribute mainly to the effect of the conservative Y217F substitution, while the less conservative Y217A mutation results in a larger 2.2 kcal/mol increase in Λ. We propose that the phenol group at position 217 functions both to stabilize the closed form of *Sc*OMPDC, through formation of a hydrogen bond to the substrate phosphodianion,[18,19,34] and to reduce the intrinsic kinetic barrier to this enzyme conformational change. We suggest that the effect of these mutations of Y217 on Λ is related to their effect on the rate of formation of the highly organized intraloop clamping interaction between the -CH_2OH side chain of Ser154 and the amide side chain of Gln215, which sits close to the phenol side chain of Y217 (Figure 4).[18,34]

■ CONCLUDING REMARK

The simplest interpretation of these results is that the large conformational change of OMPDC is necessary to lock OMP and FOMP into catalytically active caged Michaelis complexes. We have no evidence that this conformational change is coupled in any way to the decarboxylation step of the enzyme-

DOI: 10.1021/acs.biochem.5b00591
Biochemistry 2015, 54, 4555−4564

bound substrate. The steady-state kinetic parameters from Table 1 were obtained by the direct determination of decarboxylation reaction velocities. In several cases, the barrier to a nonchemical step, which we propose is an enzyme conformational change, was shown to control the observed reaction barrier. In these cases, the steady-state kinetic parameters were used to estimate the rate and equilibrium constants for this conformational change (Table 2). It would be interesting to examine the changes in the nuclear magnetic resonance[48−50] or fluorescence[51,52] spectral properties of *Sc*OMPDC during turnover of FOMP, to obtain an independent estimate of the kinetic and thermodynamic barriers to this enzyme conformational change.

AUTHOR INFORMATION

Corresponding Author

*E-mail: jrichard@buffalo.edu. Telephone: (716) 645-4232. Fax: (716) 645-6963.

Funding

This work was funded by National Institutes of Health Grant GM39754 (to J.P.R.) and Grant GM65155 (to J.A.G.).

Notes

The authors declare no competing financial interest.

ABBREVIATIONS

*Sc*OMPDC, orotidine 5′-monophosphate decarboxylase from *S. cerevisiae*; OMP, orotidine 5′-monophosphate; UMP, uridine 5′-monophosphate; FOMP, 5-fluoroorotidine 5′-monophosphate; FUMP, 5-fluorouridine 5′-monophosphate; BMP, 6-hydroxyuridine 5′-monophosphate; EO, 1-(β-D-erythrofuranosyl)orotic acid; EU, 1-(β-D-erythrofuranosyl)-uracil; FEO, 1-(β-D-erythrofuranosyl)-5-fluoroorotic acid; FEU, 1-(β-D-erythrofuranosyl)-5-fluorouracil; MOPS, 3-(*N*-morpholino)propanesulfonic acid; PDB, Protein Data Bank.

REFERENCES

(1) Miller, B. G., and Wolfenden, R. (2002) Catalytic proficiency: the unusual case of OMP decarboxylase. *Annu. Rev. Biochem. 71*, 847−885.

(2) Radzicka, A., and Wolfenden, R. (1995) A proficient enzyme. *Science 267*, 90−93.

(3) Tsang, W.-Y., Wood, B. M., Wong, F. M., Wu, W., Gerlt, J. A., Amyes, T. L., and Richard, J. P. (2012) Proton Transfer from C-6 of Uridine 5′-Monophosphate Catalyzed by Orotidine 5′-Monophosphate Decarboxylase: Formation and Stability of a Vinyl Carbanion Intermediate and the Effect of a 5-Fluoro Substituent. *J. Am. Chem. Soc. 134*, 14580−14594.

(4) Amyes, T. L., Ming, S. A., Goldman, L. M., Wood, B. M., Desai, B. J., Gerlt, J. A., and Richard, J. P. (2012) Orotidine 5′-monophosphate decarboxylase: Transition state stabilization from remote protein-phosphodianion interactions. *Biochemistry 51*, 4630−4632.

(5) Toth, K., Amyes, T. L., Wood, B. M., Chan, K., Gerlt, J. A., and Richard, J. P. (2010) Product Deuterium Isotope Effects for Orotidine 5′-Monophosphate Decarboxylase: Effect of Changing Substrate and Enzyme Structure on the Partitioning of the Vinyl Carbanion Reaction Intermediate. *J. Am. Chem. Soc. 132*, 7018−7024.

(6) Amyes, T. L., Wood, B. M., Chan, K., Gerlt, J. A., and Richard, J. P. (2008) Formation and Stability of a Vinyl Carbanion at the Active Site of Orotidine 5′-Monophosphate Decarboxylase: pK_a of the C-6 Proton of Enzyme-Bound UMP. *J. Am. Chem. Soc. 130*, 1574−1575.

(7) Toth, K., Amyes, T. L., Wood, B. M., Chan, K., Gerlt, J. A., and Richard, J. P. (2007) Product Deuterium Isotope Effect for Orotidine 5′-Monophosphate Decarboxylase: Evidence for the Existence of a Short-Lived Carbanion Intermediate. *J. Am. Chem. Soc. 129*, 12946−12947.

(8) Goryanova, B., Amyes, T. L., Gerlt, J. A., and Richard, J. P. (2011) OMP Decarboxylase: Phosphodianion Binding Energy Is Used To Stabilize a Vinyl Carbanion Intermediate. *J. Am. Chem. Soc. 133*, 6545−6548.

(9) Porter, D. J. T., and Short, S. A. (2000) Yeast Orotidine-5′-Phosphate Decarboxylase: Steady-State and Pre-Steady-State Analysis of the Kinetic Mechanism of Substrate Decarboxylation. *Biochemistry 39*, 11788−11800.

(10) Amyes, T. L., and Richard, J. P. (2013) Specificity in transition state binding: The Pauling model revisited. *Biochemistry 52*, 2021−2035.

(11) Richard, J. P., Amyes, T. L., Goryanova, B., and Zhai, X. (2014) Enzyme architecture: on the importance of being in a protein cage. *Curr. Opin. Chem. Biol. 21*, 1−10.

(12) Malabanan, M. M., Amyes, T. L., and Richard, J. P. (2010) A role for flexible loops in enzyme catalysis. *Curr. Opin. Struct. Biol. 20*, 702−710.

(13) Desai, B. J., Wood, B. M., Fedorov, A. A., Fedorov, E. V., Goryanova, B., Amyes, T. L., Richard, J. P., Almo, S. C., and Gerlt, J. A. (2012) Conformational changes in orotidine 5′-monophosphate decarboxylase: A structure-based explanation for how the 5′-phosphate group activates the enzyme. *Biochemistry 51*, 8665−8678.

(14) Wood, B. M., Amyes, T. L., Fedorov, A. A., Fedorov, E. V., Shabila, A., Almo, S. C., Richard, J. P., and Gerlt, J. A. (2010) Conformational changes in orotidine 5′-monophosphate decarboxylase: "Remote" residues that stabilize the active conformation. *Biochemistry 49*, 3514−3516.

(15) Toth, K., Amyes, T. L., Wood, B. M., Chan, K. K., Gerlt, J. A., and Richard, J. P. (2009) An Examination of the Relationship between Active Site Loop Size and Thermodynamic Activation Parameters for Orotidine 5′-Monophosphate Decarboxylase from Mesophilic and Thermophilic Organisms. *Biochemistry 48*, 8006−8013.

(16) Wolfenden, R. (1974) Enzyme catalysis. Conflicting requirements of substrate access and transition state affinity. *Mol. Cell. Biochem. 3*, 207−211.

(17) Richard, J. P., Zhai, X., and Malabanan, M. M. (2014) Reflections on the catalytic power of a TIM-barrel. *Bioorg. Chem. 57*, 206−212.

(18) Miller, B. G., Hassell, A. M., Wolfenden, R., Milburn, M. V., and Short, S. A. (2000) Anatomy of a proficient enzyme: the structure of orotidine 5′-monophosphate decarboxylase in the presence and absence of a potential transition state analog. *Proc. Natl. Acad. Sci. U. S. A. 97*, 2011−2016.

(19) Goldman, L. M., Amyes, T. L., Goryanova, B., Gerlt, J. A., and Richard, J. P. (2014) Enzyme Architecture: Deconstruction of the Enzyme-Activating Phosphodianion Interactions of Orotidine 5′-Monophosphate Decarboxylase. *J. Am. Chem. Soc. 136*, 10156−10165.

(20) Zhai, X., Amyes, T. L., and Richard, J. P. (2014) Enzyme Architecture: Remarkably Similar Transition States for Triosephosphate Isomerase-Catalyzed Reactions of the Whole Substrate and the Substrate in Pieces. *J. Am. Chem. Soc. 136*, 4145−4148.

(21) Go, M. K., Amyes, T. L., and Richard, J. P. (2009) Hydron Transfer Catalyzed by Triosephosphate Isomerase. Products of the Direct and Phosphite-Activated Isomerization of [1-^{13}C]-Glycolaldehyde in D_2O. *Biochemistry 48*, 5769−5778.

(22) Amyes, T. L., and Richard, J. P. (2007) Enzymatic catalysis of proton transfer at carbon: activation of triosephosphate isomerase by phosphite dianion. *Biochemistry 46*, 5841−5854.

(23) Richard, J. P. (2012) A Paradigm for Enzyme-Catalyzed Proton Transfer at Carbon: Triosephosphate Isomerase. *Biochemistry 51*, 2652−2661.

(24) Tsang, W.-Y., Amyes, T. L., and Richard, J. P. (2008) A Substrate in Pieces: Allosteric Activation of Glycerol 3-Phosphate Dehydrogenase (NAD^+) by Phosphite Dianion. *Biochemistry 47*, 4575−4582.

(25) Reyes, A. C., Zhai, X., Morgan, K. T., Reinhardt, C. J., Amyes, T. L., and Richard, J. P. (2015) The Activating Oxydianion Binding Domain for Enzyme-Catalyzed Proton Transfer, Hydride Transfer and

DOI: 10.1021/acs.biochem.5b00591
Biochemistry 2015, 54, 4555−4564

Decarboxylation: Specificity and Enzyme Architecture. *J. Am. Chem. Soc. 137*, 1372−1382.
(26) Reyes, A. C., Koudelka, A. P., Amyes, T. L., and Richard, J. P. (2015) Enzyme Architecture: Optimization of Transition State Stabilization from a Cation−Phosphodianion Pair. *J. Am. Chem. Soc. 137*, 5312−5315.
(27) Wood, B. M., Chan, K. K., Amyes, T. L., Richard, J. P., and Gerlt, J. A. (2009) Mechanism of the Orotidine 5′-Monophosphate Decarboxylase-Catalyzed Reaction: Effect of Solvent Viscosity on Kinetic Constants. *Biochemistry 48*, 5510−5517.
(28) Van Vleet, J. L., Reinhardt, L. A., Miller, B. G., Sievers, A., and Cleland, W. W. (2008) Carbon isotope effect study on orotidine 5′-monophosphate decarboxylase: support for an anionic intermediate. *Biochemistry 47*, 798−803.
(29) Goryanova, B., Goldman, L. M., Amyes, T. L., Gerlt, J. A., and Richard, J. P. (2013) Role of a Guanidinium Cation−Phosphodianion Pair in Stabilizing the Vinyl Carbanion Intermediate of Orotidine 5′-Phosphate Decarboxylase-Catalyzed Reactions. *Biochemistry 52*, 7500−7511.
(30) Goryanova, B., Spong, K., Amyes, T. L., and Richard, J. P. (2013) Catalysis by Orotidine 5′-Monophosphate Decarboxylase: Effect of 5-Fluoro and 4′-Substituents on the Decarboxylation of Two-Part Substrates. *Biochemistry 52*, 537−546.
(31) Stein, R. L., Fujihara, H., Quinn, D. M., Fischer, G., Kuellertz, G., Barth, A., and Schowen, R. L. (1984) Transition-state structural features for anilide hydrolysis from β-deuterium isotope effects. *J. Am. Chem. Soc. 106*, 1457−1461.
(32) Chan, K. K., Wood, B. M., Fedorov, A. A., Fedorov, E. V., Imker, H. J., Amyes, T. L., Richard, J. P., Almo, S. C., and Gerlt, J. A. (2009) Mechanism of the Orotidine 5′-Monophosphate Decarboxylase-Catalyzed Reaction: Evidence for Substrate Destabilization. *Biochemistry 48*, 5518−5531.
(33) Gross, A., Abril, O., Lewis, J. M., Geresh, S., and Whitesides, G. M. (1983) Practical synthesis of 5-phospho-D-ribosyl α-1-pyrophosphate (PRPP): enzymatic routes from ribose 5-phosphate or ribose. *J. Am. Chem. Soc. 105*, 7428−7435.
(34) Barnett, S. A., Amyes, T. L., Wood, B. M., Gerlt, J. A., and Richard, J. P. (2008) Dissecting the Total Transition State Stabilization Provided by Amino Acid Side Chains at Orotidine 5′-Monophosphate Decarboxylase: A Two-Part Substrate Approach. *Biochemistry 47*, 7785−7787.
(35) Gasteiger, E., Hoogland, C., Gattiker, A., Duvaud, S., Wilkins, M. R., Appel, R. D., and Bairoch, A., Eds. (2005) *Protein Identification and Analysis Tools on the ExPASy Server*, Humana Press Inc., Totowa, NJ.
(36) Gasteiger, E., Gattiker, A., Hoogland, C., Ivanyi, I., Appel, R. D., and Bairoch, A. (2003) ExPASy: The proteomics server for in-depth protein knowledge and analysis. *Nucleic Acids Res. 31*, 3784−3788.
(37) Barnett, S. A. (2009) Studies on the Mechanism of Action of Orotidine 5′-Monophosphate Decarboxylase. Ph.D. Thesis, University at Buffalo, Buffalo, NY.
(38) Miller, B. G., Butterfoss, G. L., Short, S. A., and Wolfenden, R. (2001) Role of Enzyme-Ribofuranosyl Contacts in the Ground State and Transition State for Orotidine 5′-Phosphate Decarboxylase: A Role for Substrate Destabilization? *Biochemistry 40*, 6227−6232.
(39) Blacklow, S. C., Raines, R. T., Lim, W. A., Zamore, P. D., and Knowles, J. R. (1988) Triosephosphate isomerase catalysis is diffusion controlled. *Biochemistry 27*, 1158−1165.
(40) Marcus, R. A. (1969) Unusual Slopes of Free Energy Plots in Kinetics. *J. Am. Chem. Soc. 91*, 7224−7225.
(41) Marcus, R. A. (1968) Theoretical Relations among Rate Constants, Barriers, and Brønsted Slopes of Chemical Reactions. *J. Phys. Chem. 72*, 891−899.
(42) Richard, J. P., and Williams, K. B. (2007) A Marcus Treatment of Rate Constants for Protonation of Ring-Substituted α-Methoxystyrenes: Intrinsic Reaction Barriers and the Shape of the Reaction Coordinate. *J. Am. Chem. Soc. 129*, 6952−6961.
(43) Richard, J. P., Amyes, T. L., and Williams, K. B. (1998) Intrinsic barriers to the formation and reaction of carbocations. *Pure Appl. Chem. 70*, 2007−2014.
(44) Richard, J. P., Amyes, T. L., and Toteva, M. M. (2001) Formation and Stability of Carbocations and Carbanions in Water and Intrinsic Barriers to Their Reactions. *Acc. Chem. Res. 34*, 981−988.
(45) Richard, J. P., and Nagorski, R. W. (1999) Mechanistic Imperatives for Catalysis of Aldol Addition Reactions: Partitioning of the Enolate Intermediate between Reaction with Bronsted Acids and the Carbonyl Group. *J. Am. Chem. Soc. 121*, 4763−4770.
(46) Guthrie, J. P. (1991) Rate-equilibrium correlations for the aldol condensation: an analysis in terms of Marcus theory. *J. Am. Chem. Soc. 113*, 7249−7255.
(47) Guthrie, J. P., and Guo, J. (1996) Intramolecular Aldol Condensations: Rate And Equilibrium Constants. *J. Am. Chem. Soc. 118*, 11472−11487.
(48) Massi, F., Wang, C., and Palmer, A. G., III. (2006) Solution NMR and computer simulation studies of active site loop motion in triosephosphate isomerase. *Biochemistry 45*, 10787−10794.
(49) Loria, J. P., Berlow, R. B., and Watt, E. D. (2008) Characterization of enzyme motions by solution NMR relaxation dispersion. *Acc. Chem. Res. 41*, 214−221.
(50) Rozovsky, S., Jogl, G., Tong, L., and McDermott, A. E. (2001) Solution-state NMR investigations of triosephosphate isomerase active site loop motion: Ligand release in relation to active site loop dynamics. *J. Mol. Biol. 310*, 271−280.
(51) Hernandez-Alcantara, G., Rodriguez-Romero, A., Reyes-Vivas, H., Peon, J., Cabrera, N., Ortiz, C., Enriquez-Flores, S., De la Mora-De la Mora, I., and Lopez-Velazquez, G. (2008) Unraveling the mechanisms of tryptophan fluorescence quenching in the triosephosphate isomerase from Giardia lamblia. *Biochim. Biophys. Acta, Proteins Proteomics 1784*, 1493−1500.
(52) Desamero, R., Rozovsky, S., Zhadin, N., McDermott, A., and Callender, R. (2003) Active Site Loop Motion in Triosephosphate Isomerase: T-Jump Relaxation Spectroscopy of Thermal Activation. *Biochemistry 42*, 2941−2951.

DOI: 10.1021/acs.biochem.5b00591
Biochemistry 2015, 54, 4555−4564